Ailanthone suppresses the activity of human colorectal cancer cells through the STAT3 signaling pathway

HAIXIANG DING, XIUCHONG YU and ZHILONG YAN

Department of Gastrointestinal Surgery, The Affiliated Hospital of Medical School of Ningbo University and Ningbo First Hospital, Ningbo, Zhejiang 315010, P.R. China

Received October 26, 2021; Accepted December 3, 2021

DOI: 10.3892/ijmm.2021.5076

Abstract. Ailanthone (AIL) is a major quassinoid extracted from the Chinese medicinal herb, *Ailanthus altissima*, which has been reported to exert anti-proliferative effects on various cancer cells. The present study aimed to investigate the anti-tumor effects of AIL on HCT116 and SW620 colon cancer cells, and to analyze the underlying molecular mechanisms. CCK-8 assay was used to detect cell viability. Furthermore, colony formation and Transwell assays, and flow cytometry were used to examine the effects of AIL on cell proliferation, apoptosis and migration. Finally, the expression levels of cell cycle control proteins, and caspase and Bcl-2 family-related proteins involved in the regulation of apoptosis, as well as those of cell migration- and pathway-related proteins were examined using western blot analysis. Reverse transcription-quantitative PCR was used to quantitatively analyze the changes in the JAK and STAT3 gene levels in each group. The *in vitro* cell function tests revealed that AIL inhibited the proliferation and migration, and induced the apoptosis and cell cycle arrest of HCT116 and SW620 cells. It was further found exerted these effects via the JAK/STAT3 signaling pathway, as well as through caspase and Bcl-2 family proteins. On the whole, the present study demonstrates that AIL suppresses the activity of colon cancer cells via the STAT3 pathway.

Correspondence to: Dr Zhilong Yan, Department of Gastrointestinal Surgery, The Affiliated Hospital of Medical School of Ningbo University and Ningbo First Hospital, 9 Liuting Street, Ningbo, Zhejiang 315010, P.R. China
E-mail: yanzhilong@nbu.edu.cn

Abbreviations: AIL, Ailanthone; CRC, colorectal cancer; JAK, Janus kinase; STAT3, signal transducer and activator of transcription 3; EMT, epithelial-mesenchymal transition; CDKs, cyclin-dependent protein kinases; CKIs, CDK inhibitors; CCK-8, Cell Counting Kit-8; Bcl-2, B cell lymphoma-2; Bax, Bcl-2-associated X; MMPs, matrix metalloproteinases

Key words: Ailanthone, CRC, STAT3, mechanism, apoptosis, EMT

Introduction

Colorectal cancer (CRC) is the third most common type of cancer worldwide. Statistical data from 2018 indicated that there were >1.8 million new cases of CXRC worldwide, and >880,000 patients succumbed to the disease. This accounts for 10.2 and 9.2% of new cancer patients and cancer-related deaths, respectively (1). Chemotherapy is one of the main treatments for CRC. However, it is associated with several side-effects, such as nephrotoxicity, cardiotoxicity, gastrointestinal reactions, neurotoxicity and bone marrow suppression. Long-term multiple chemotherapy often leads to the accumulation of toxic side-effects and to an increase in drug resistance, which is the main reason for the failure of chemotherapy (2). At present, there is still a lack of effective chemotherapeutic drugs with low toxicity. As the source of numerous anticancer agents, the extracts of natural plants exert minimal side-effects and can prevent resistance to chemotherapeutic drugs to a certain extent (3).

Ailanthus altissima is a plant of the genus *Ailanthus* in the family Simaroubaceae, commonly known as tree of heaven (4). It can be found worldwide, essentially in countries with a temperate climate. As a type of traditional Chinese medicine, it has a long history of use in China. It can be used in the treatment of diseases, such as inflammation, malaria, allergy, tuberculosis, ulcers, amoebiasis, viral infections, HIV and cancer (5). The medicinal ingredient is considered to be Ailanthone (AIL), a water-soluble quassinoid, and is mainly extracted from the bark of this plant (chemical structure shown in Fig. 1A). AIL was first isolated in 1955 (6) and its structure was clarified in the early 1980s (7). A number of *in vitro* studies have demonstrated that AIL exerts anticancer effects on a variety of cancer cells, such as lung cancer (8), melanoma (9), bladder (10), stomach (11), prostate (12) and liver cancer (13), etc. In these tumor cells, AIL plays an anticancer role mainly through the inhibition of proliferation, the induction of apoptosis and autophagy, and by mediating a variety of molecular targets and signaling pathways to exert anticancer effects.

To date, at least to the best of our knowledge, there is no relevant research available the effects of AIL on CRC. Therefore, the present study used the HCT116 and SW620 CRC cells to observe the effects of AIL on the proliferation, apoptosis and cell cycle distribution of AIL these cells. Moreover,

in order to explore the specific molecular mechanisms of AIL, the changes in the expression of cell cycle-related proteins and apoptosis regulatory proteins were examined. It was also found that AIL inhibit the activation of the Janus kinase (JAK)/signal transducer and activator of transcription (STAT)3 signaling pathway. These findings clarify the molecular mechanisms of AIL against CRC cells to a certain extent, and provide the experimental and theoretical basis for the application of AIL in the treatment of CRC.

Materials and methods

Materials, antibodies and reagents. AIL was extracted and isolated from *Ailanthus altissima*. The AIL sample (purity ≥98%) was provided by Shanghai Yiyan Biotechnology Co., Ltd. 5-Fluorouracil (5-FU) was obtained from MedChemExpress. The Cell Mitochondria Isolation kit (cat no. C3601) was purchased from the Beyotime Institute of Biotechnology. All the antibodies used in the present study were as follows: Antibodies for mouse polyclonal β-actin (cat no. bsm-33036M), mouse monoclonal B-cell lymphoma-2 (Bcl-2; cat no. bsm-33411M), rabbit polyclonal Bcl-2-associated X protein (Bax; cat no. bs-0127R), rabbit polyclonal cyclin-dependent protein kinase 1 (CDK1; cat no. bs-1341R), rabbit polyclonal Cyclin B1 (cat no. bs-0572R), rabbit polyclonal STAT3 (cat no. bs-55208R), rabbit polyclonal E-cadherin (cat no. bs-10009R), rabbit polyclonal N-cadherin (cat no. bs-1172R), rabbit polyclonal Vimentin (cat no. bs-8533R), rabbit polyclonal cytochrome *c* (cat no. bs-0013R), rabbit polyclonal voltage-dependent anion-selective channel (VDAC; cat no. bs-7647R) were purchased from BIOSS. The antibodies for rabbit monoclonal caspase-3 (cat no. 14220), mouse monoclonal caspase-9 (cat no. 9508), rabbit monoclonal PARP (cat no. 9532), horseradish peroxidase (HRP)-conjugated goat anti-mouse (cat no. 91196) immunoglobulin (Ig)G were obtained from Cell Signaling Technology, Inc., and goat anti-rabbit (cat no. AS014) immunoglobulin (Ig)G was purchased from ABclonal Biotech Co., Ltd.

Cells and cell culture. The human CRC cell lines, HCT116 and SW620 (cat. no. TCHu 99 and TCHu101), were obtained from The Cell Bank of Type Culture Collection of The Chinese Academy of Sciences. The human normal colonic epithelial cell line, NCM460, was also obtained from The Cell Bank of Type Culture Collection of The Chinese Academy of Sciences. The HCT116 and NCM460 cells were cultured in RPMI-1640 medium supplemented with 10% FBS and 1% PS in a humidified incubator containing 5% CO_2 and 95% air at 37˚C for cell subculture and all the experiments. Under the same conditions, the SW620 cells were cultured in L-15 medium supplemented with 10% FBS and 1% PS. Stock solutions of AIL were prepared in DMSO, and stored at -20˚C. Prior to use, stock solutions were immediately diluted to the required concentration with complete medium; the terminal concentration of DMSO in the culture medium was ≤0.1%.

Cell viability assay. The Cell Counting Kit-8 (CCK-8) assay obtained from MedChemExpress (cat no. HY-K0301) was used to measure cell viability. 5-FU was used in the positive control. The NCM460, HCT116, SW620 cells in the exponential growth phase ($5x10^3$ cells/well) were seeded and cultured in 96-well plates for 24 h, and were then treated with AIL (0.2, 0.4, 0.8, 1.6 and 3.2 μM) or 5-FU (0.2, 0.4, 0.8, 1.6 and 3.2 μM) for 24, 48, 72 and 96 h at 37˚C; each group was analyzed 4 times. Subsequently, 10 μl CCK-8 solution were added to each well. Following incubation for 3 h at 37˚C, the optical density was measured at a wavelength of 450 nm using a microplate reader (SpectraMax M5; Molecular Devices, LLC). The relative cell viability was calculated based on the optical density value. Prism 9.2 (GraphPad Software, Inc.) was then used to calculate the IC50 value based on the relative cell viability.

Transwell assay. A 0.4 μm Transwell assay (Costar; Corning, Inc.) was used to assess cell migration. In brief, $6x10^4$ CRC cells (HCT116 and SW620) were seeded in the upper side of the chamber with non-serum culture medium. The lower chamber was filled with 500 μl complete culture medium. The chamber was then placed in a humidified incubator at 37˚C for 24 h. The CRC cells were treated with 0.4 μM AIL for 48 h, and the traversed cells (the cells in the lower chamber) were then stained with crystal violet (Sinopharm Group Co., Ltd.) at room temperature for 3 h and counted microscopically using a binocular microscope (Olympus CX23). Five fields were randomly selected for calculation of relative migration.

Cell apoptosis analysis. The Annexin-V-FITC Apoptosis Detection kit [Hangzhou Multi Sciences (Lianke) Biotech Co.] was used to analyze cell apoptosis. Following treatment with AIL (0.2 and 0.4 μM) for 48 h, $1x10^5$ SW620 and HCT116 cells were collected from each sample. The cells were suspended in a binding buffer containing 10 μl Annexin-V-FITC, and then incubated at room temperature in the dark for 30 min. Subsequently, 5 μl PI and 200 ml ice-cold PBS were added, and the samples were immediately analyzed using a FACSscan flow cytometer (CytoFLEX; Beckman Coulter, Inc.). $FITC^+$ and PI^- cells were considered apoptotic.

JC-1 staining. The HCT116 and SW620 cells were seeded in a 6-well plate at a density of $1x10^5$ cells/well for 12 h, and treated with various concentrations of AIL (0, 0.2 and 0.4 μM) for 48 h. The cells were then collected and resuspended in JC-1 (Solebold) for 30 min at 37˚C in the dark. JC-1 is a type of dye that targets the mitochondrion and is used as a reporter for membrane potential. It has two states: Monomer and multimer. In normal cells, JC-1 enters the mitochondria and forms red fluorescent multimers due to the increase in the concentration. In apoptotic cells, the mitochondrial membrane potential is lost, JC-1 is released from the mitochondria, the concentration decreases, and it turns into a green fluorescent monomer form. Therefore, the changes in mitochondrial membrane potential were quantified by detecting green and red fluorescence using a flow cytometer (CytoFLEX; Beckman Coulter, Inc.).

Cell cycle distribution analysis. The cells were seeded in a 6-well plate at a density of $1x10^6$/ml and treated with AIL (0.2 and 0.4 μM) for 48 h. Following treatment, the cells were collected and resuspended in 0.5 ml PBS, fixed with 70% cold ethanol at -20˚C overnight, and then mixed with 1 ml DNA staining solution and incubated at 0˚C for 30 min. The cell

cycle distribution was then analyzed using a flow cytometer (CytoFLEX; Beckman Coulter, Inc.).

Isolation of mitochondria from cells. The cells were collected and washed with PBS, and were pelleted by centrifugation at 600 x g for 5 min at 4˚C. After the supernatant was discarded, 1.5 ml mitochondrial separation reagent (cat no. SM0020; Beijing Solarbio Science & Technology Co., Ltd.) was added to resuscitate the cells, and the cells were then placed in an ice bath for 15 min. The cells were homogenized 15 times using a homogenizer (cat no. YA0856; Beijing Solarbio Science & Technology Co., Ltd.), and the cell homogenate was then centrifuged at 800 x g for 10 min at 4˚C. As a final step, the supernatant was transferred to another tube and centrifuged again at 11,000 x g for 10 min at 4˚C. Finally, the precipitate obtained was the separated mitochondria.

Western blot analysis. Following treatment with AIL (0.2, 0.4, 0.8, 1.6 and 3.2 μM) for 48 h at 37˚C, the HCT116 and SW620 cells were washed twice with ice-cold PBS and suspended in lysis buffer (cat no. R0020; Solarbio Biotech Co., Ltd.) on ice for 30 min. The lysates were then cleared by centrifugation at 12,000 x g for 15 min at 4˚C. Subsequently, the Bradford protein assay kit (cat no. P0006; Beyotime Biotech Co., Ltd.) was used to measure the total protein concentration of each sample. A total of 50 μg protein samples from each group were separated by 12% SDS-PAGE and were then transferred onto polyvinylidene fluoride membranes (MilliporeSigma). The membranes were then blocked with 5% non-fat dry milk dissolved in TBS containing 0.05% Tween-20 (TBST) at room temperature for 1 h, and were then washed three times with TBST. Subsequently, the membranes were incubated with the primary antibodies (1:1,500) overnight at 4˚C. After washing three times with TBST, the membranes were incubated with HRP-conjugated goat anti-mouse (1:2,000) or anti-rabbit (1:2,000) IgG secondary antibodies at room temperature for 1 h. The immunoreactive bands were visualized with chemiluminescent substrates (cat no. K-12045-D50; Advansta Scientific, Inc.) using an X-ray film processor (Clinx ChemiScope 3000Mini; Clinx Science Instruments Co., Ltd.). β-actin and VDAC were used as loading controls. The experiment was independently repeated three times, and ImageJ software (version 1.8.0; National Institutes of Health, USA) was used for densitometric analysis of the protein bands.

Total RNA extraction and reverse transcription-quantitative PCR (RT-qPCR). To detect the relative expression levels of JAK and STAT3, RT-qPCR was performed. Briefly, the HCT116 and SW620 cells were treated with various concentrations (0, 0.2 and 0.4 μM) of AIL for 48 h. Total RNA from was then extracted from the CRC cell lines using TRIzol® reagent (Invitrogen; Thermo Fisher Scientific, Inc.) as per the manufacturer's instructions. The extracted RNA was then converted into cDNA using the GoScript Reverse Transcription System (Promega Corporation) using following the steps: i) Denaturation of the template into single strands; ii) annealing (25˚C, 5 min) of primers to each original strand for new strand synthesis; and iii) extension (43˚C, 55 min) of the new DNA strands from the primers. Subsequently, qPCR was performed using GoTaq® 2-Step RT-qPCR System (Promega Corporation) by applying a Stratagene MX3005P qPCR System (Agilent Technologies, Inc.) using 5 μl cDNA. The primer sequences used were as follows: JAK forward, 5'-TCTGGGGAGTATGTTGCAGAA-3' and reverse, 5'-AGACATGGTTGGGTGGATACC-3'; STAT3 forward, 5'-GAGAAGGACATCAGCGGTAAG-3' and reverse, 5'-CAGTGGAGACACCAGGATATTG-3'; and human GAPDH (used as an internal control) forward, 5'-AAGGTGAAGGTCGGAGTCAA-3' and reverse, 5'-AATGAAGGGGTCATTGATGG-3'. ΔΔCq values were calculated to reflect the expression of JAK and STAT3 (14).

Statistical analysis. All data were analyzed using SPSS software (version 18.0; SPSS, Inc.). All statistical graphs are constructed using Prism 9.2 (GraphPad Software, Inc.). All the experiments were conducted in triplicate, and all data are expressed as the mean ± SD. An unpaired Student's t-test was used to compare differences between two groups. The statistical significance of the differences among more than two groups were analyzed using one-way ANOVA and a Tukey's post hoc test. $P<0.05$ was considered to indicate a statistically significant difference.

Results

AIL inhibits CRC cell proliferation. CCK-8 assay was used to detect the effects of AIL on the growth of the HCT116, SW620 and NCM460 cells treated with AIL (0-3.2 μM) or 5-FU (0-3.2 μM) for 24, 48, 72 and 96 h at 37˚C. AIL inhibited the viability of these three cells in a dose- and time-dependent manner (Fig. 1B-D). The half maximal inhibitory concentration (IC50) values of AIL in the HCT116 cells at 24, 48 72 and 96 h were 1.79±0.139, 1.147±0.056, 0.603±0.067 and 0.449±0.021 μM, respectively. The half maximal inhibitory concentration (IC50) values of AIL in the SW620 cells at 24, 48 72 and 96 h were 3.255±0.479, 2.333±0.23, 1.01±0.079 and 0.834±0.066 μM, respectively. Cells treated with 5-FU were considered as the positive control group; 5-FU also inhibited the growth of these two CRC cells in a dose- and time-dependent manner (Fig. 1E and F). The IC50 values of 5-FU in the HCT116 cells at 24, 48 72 and 96 h were 4.511±0.572, 1.691±0.355, 0.576±0.045 and 0.358±0.011 μM, respectively. The IC50 value of 5-FU in SW620 cells at 24, 48, 72 and 96 h were 5.666±0.259, 4.96±0.61, 3.304±1.059 and 1.065±0.144 μM, respectively. When comparing the IC50 values of these two drugs, it was found that the antitumor effect of AIL on the CRC cells was similar to that of 5-FU.

Furthermore, the cytotoxicity of AIL on normal intestinal epithelial cells NCM460 was also evaluated. The IC50 values at 24, 48, 72 and 96 h were 5.67±0.155, 3.89±0.553, 1.759±0.119 and 1.314±0.027 μM, respectively (Fig. 1D). It can be seen that in the experimental group (0.2 and 0.4 μM), AIL exerted more significant cytotoxic effects on the tumor cells than on the normal intestinal epithelial cells (Fig. 1G).

AIL inhibits colorectal cancer cell migration. Transwell assay was conducted to assess the migratory capacity of the CRC cells. As shown in Fig. 2A, the relative migration rate was significantly decreased in the AIL group compared with the control group ($P<0.01$ or $P<0.001$). By performing western blot

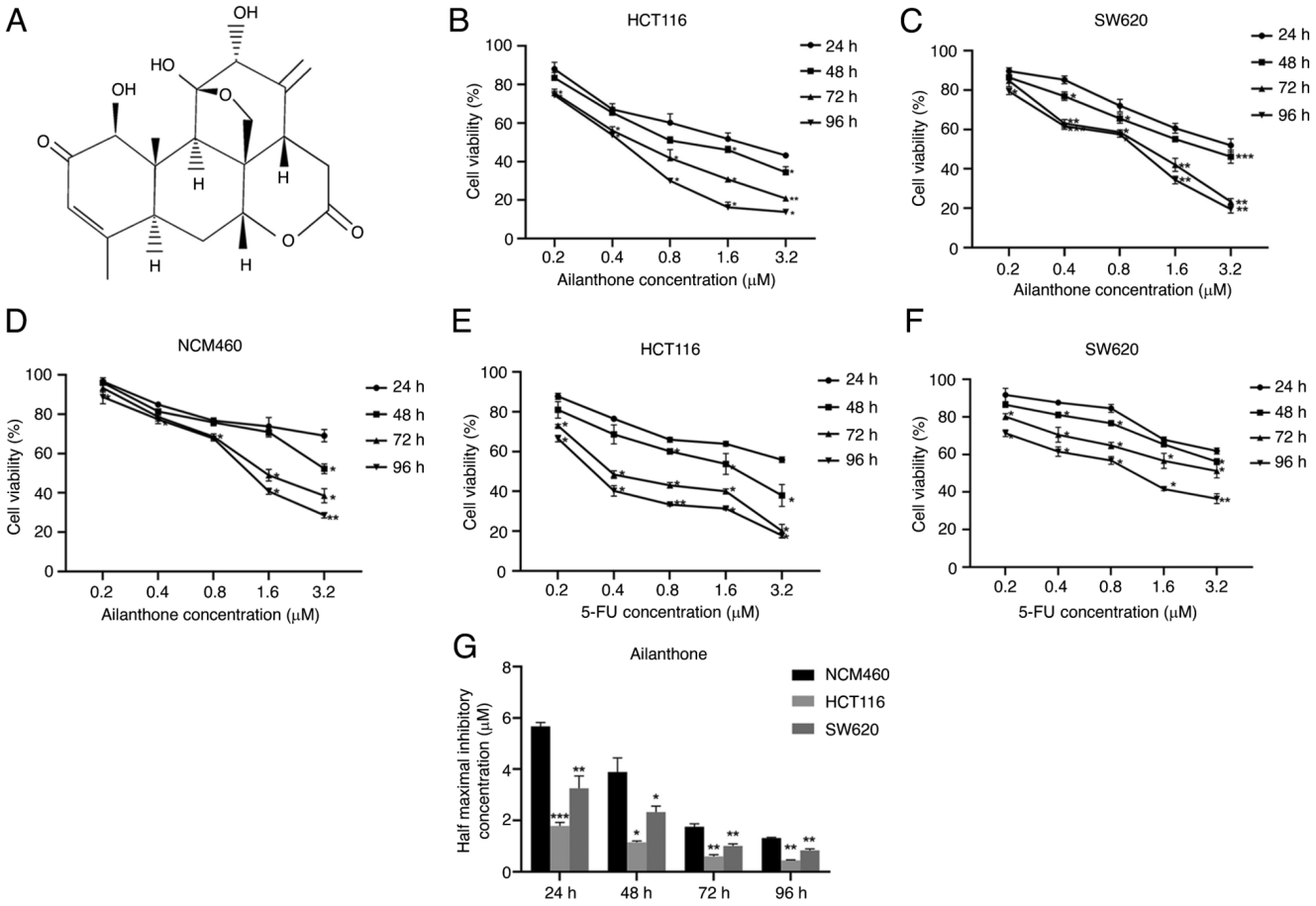

Figure 1. Growth-inhibitory effects of AIL and 5-FU on the HCT116 and SW620 cells, and the growth-inhibitory effects of AIL on the NCM460 cells. (A) Molecular structure of AIL. (B-D) AIL exerted inhibitory effects on the growth of HCT116, SW620 and NCM460 cells in a concentration- and time-dependent manner. (E and F) Effects of 5-FU induced on HCT116 and SW620 cell growth. (G) Comparison of the IC50 values of AIL in the three cell lines (HCT116, SW620 and NCM460) following treatment with AIL for different periods of time (24, 48, 72 and 96 h). Data are presented as the mean ± standard deviation, n=3. *P<0.05, **P<0.01 and ***P<0.001, vs. respective control. AIL, Ailanthone; 5-FU, 5-fluorouracil.

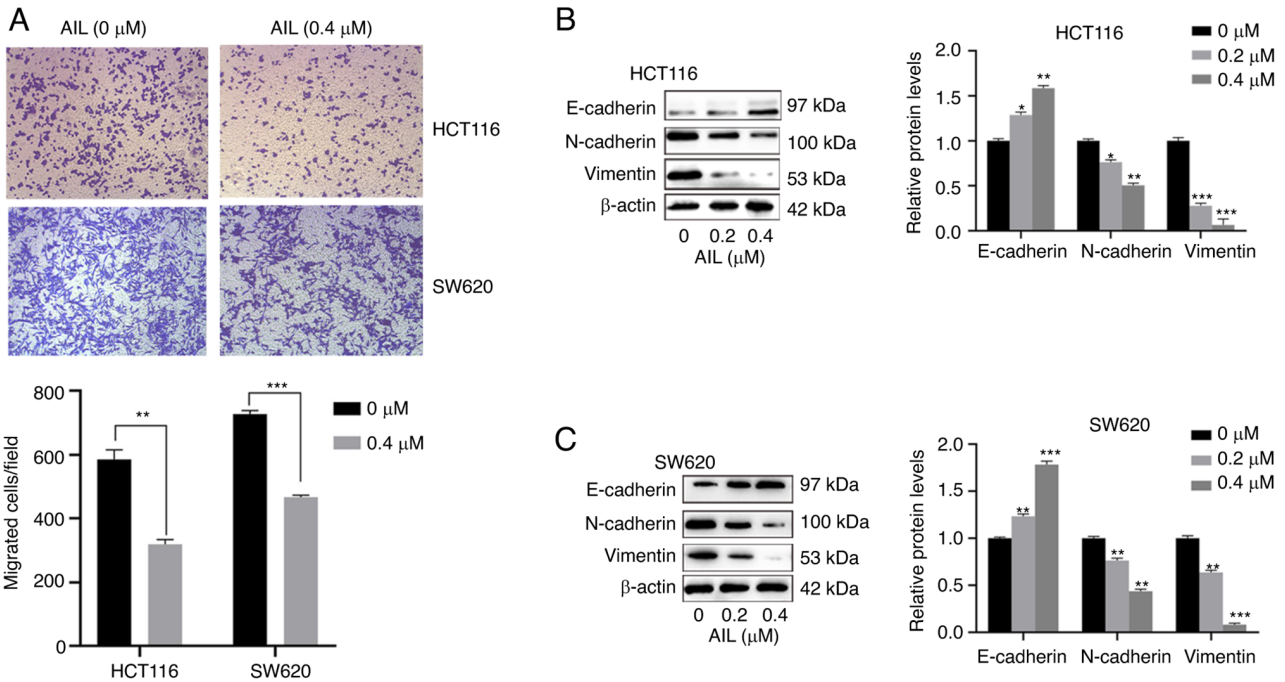

Figure 2. AIL inhibits the migration of colorectal cancer cells. (A) AIL inhibited the migration of the HCT116 and SW620 cells. (B and C) Changes in the expression of EMT-related proteins (E-cadherin, N-cadherin and Vimentin). Data are presented as the mean ± standard deviation, n=3. *P<0.05, **P<0.01 and ***P<0.001, vs. control (0 h). AIL, Ailanthone.

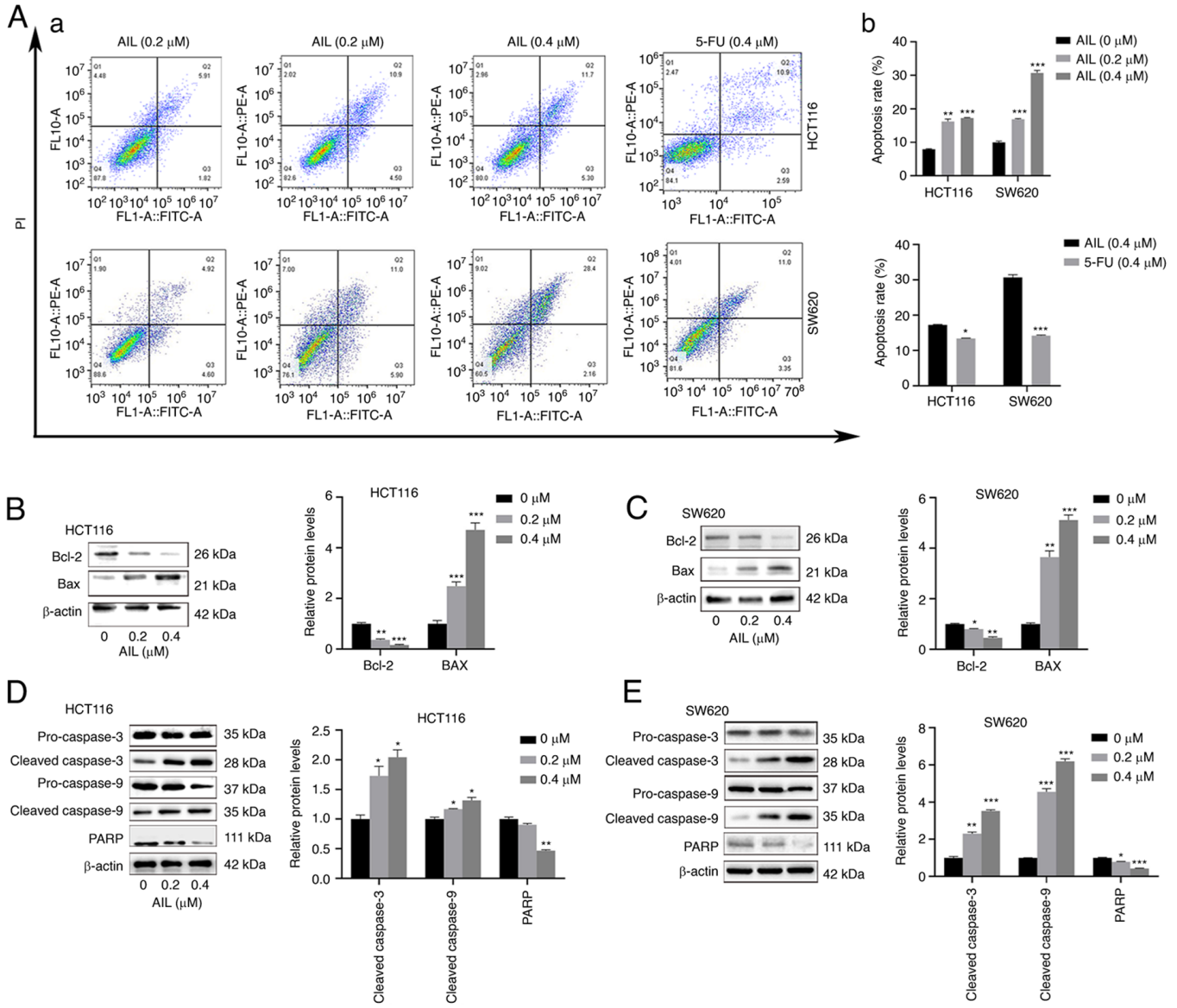

Figure 3. AIL induces caspase-dependent apoptosis. (A-a) Detection of the apoptosis of CRC cells (HCT116 and SW620) treated with AIL or 5-FU for 48 h at 37˚C. Early (lower right quadrant) and late (upper right quadrant) apoptotic cells were detected using flow cytometry. (A-b) Percentage of apoptotic cells. (B) Effects of AIL on the mitochondrial membrane potential of CRC cells. (B and C) Changes in the expression of apoptosis-related proteins (Bcl-2 and Bax). (D and E) Changes in the expression of apoptosis-related proteins (caspase-3 and -9). Data are presented as the mean ± standard deviation, n=3. *P<0.05, **P<0.01 and ***P<0.001, vs. respective control. AIL, Ailanthone; 5-FU, 5-fluorouracil; CRC, colorectal cancer.

analysis, it was found that the protein levels of N-cadherin and Vimentin were both significantly downregulated in the AIL group, as compared with the control group, while E-cadherin expression was significantly upregulated (P<0.05, P<0.01, P<0.001 or P<0.0001 Fig. 2B and C). These results demonstrated that AIL was able to suppress the migratory capacities of the CRC cells.

AIL induces caspase-dependent apoptosis. To confirm the occurrence of apoptosis, an Annexin V-FITC/PI double-staining assay was performed. As shown in Fig. 3A, the percentage of apoptotic HCT116 cells (including early and late apoptotic cells) significantly increased with the increasing AIL concentration, from 7.90±0.18 to 17.25±0.15%, while the apoptotic rate of the SW620 cells increased from 9.97±0.40 to 30.7±0.77%. It was also found that at the same concentration (0.4 μM), the apoptosis-promoting effects of AIL on the HCT116 cells (17.22±0.19%) were more prominent than those of 5-FU (13.41±0.92%). Similar results were obtained for the SW620 cells. The apoptosis induction rates of the two drugs for the SW620 cells were 30.70±0.77 and 14.22±0.15%, respectively.

In addition, compared with the control group, following 48 h of treatment with AIL (0-0.4 μM) at 37˚C, the expression level of the inhibitor of apoptosis protein, Bcl-2, in the two CRC cells was decreased, while the expression level of the apoptosis-promoting protein, Bax, was increased (Fig. 3B and C). Since caspase activation is considered a hallmark of apoptosis, western blot analysis was performed to examine caspase activation. The levels of cleaved caspase-9 and cleaved caspase-3 were significantly increased in the AIL-treated cells. The expression of the caspase cleaved

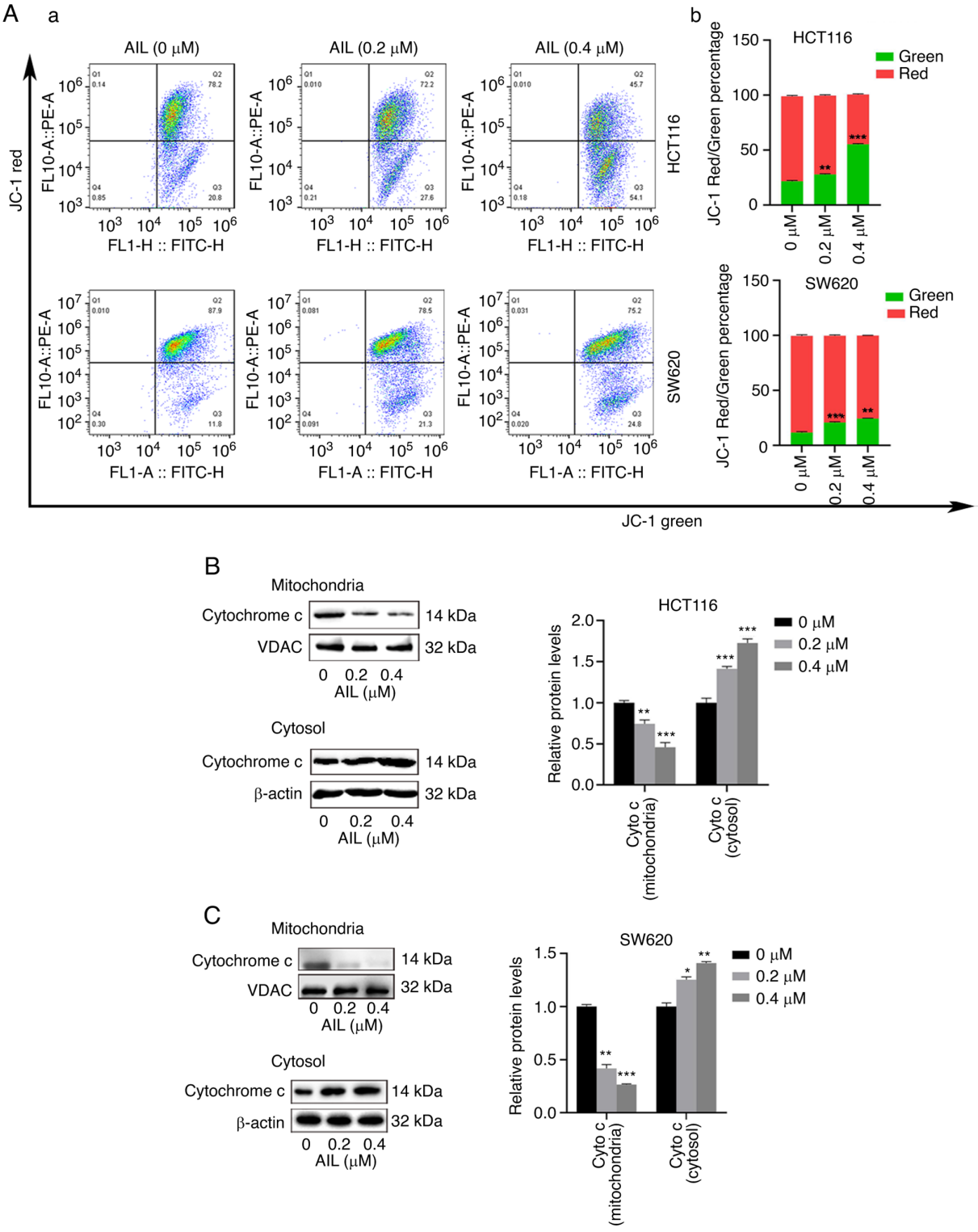

Figure 4. Effects of AIL on the mitochondrial membrane potential of colorectal cancer cells. (A-a) The red-green percentage of mitochondrial JC-1 activity was determined using flow cytometry. (A-b) Comparison of red-green ratio. (B and C) Western blot analysis revealed that the change in the distribution of cytochrome *c* from the mitochondria to the cytosol. Data are presented as the mean ± standard deviation, n=3. *P<0.05, **P<0.01 and ***P<0.001, vs. control (no treatment). AIL, Ailanthone.

substrate PARP was significantly decreased, which also indicated caspase activation (Fig. 3D and E).

AIL induces apoptosis through mitochondrial pathways. Subsequently, mitochondrial membrane potential was analyzed using JC-1 staining. As shown in Fig. 4A, the JC-1 red/green percentage in the two CRC cell lines decreased following AIL treatment.

Mitochondrial dysfunction, can subsequently lead to the release of cytochrome *c* from the mitochondria to the cytosol. The increased distribution of cytochrome *c* in the cytosol is considered to be related to the apoptosis induced by the

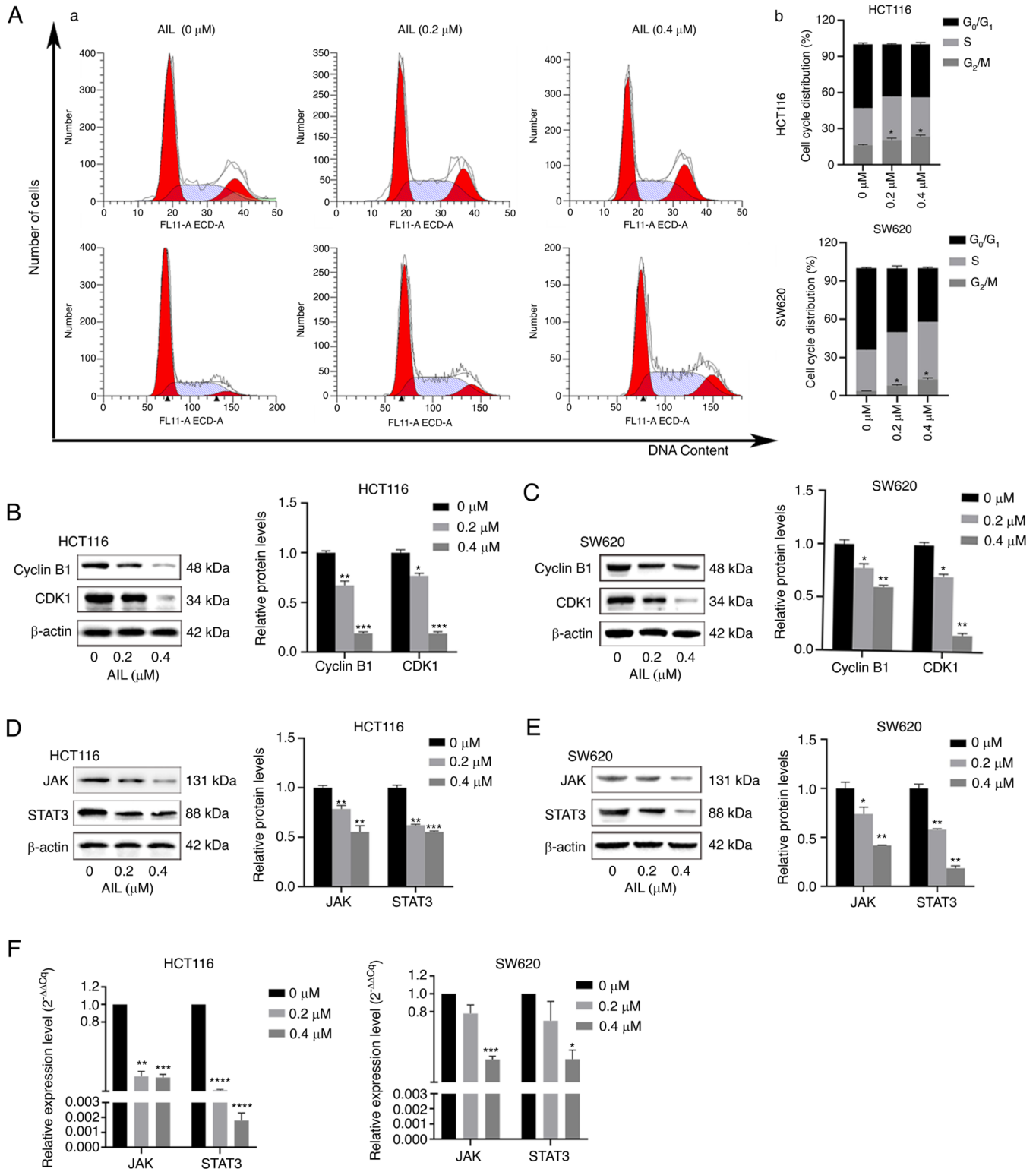

Figure 5. AIL induces cell cycle arrest and inhibits the activation of tumor-related signaling pathways. (A) Flow cytometry was used to determine the DNA content of CRC cells treated with AIL for 48 h at 37˚C. (A-a) Percentage of cells in each cell cycle phase. (A-b) Comparison of the percentage of cells in the G2/M phase. (B and C) Effect of AIL on cell cycle regulatory proteins (cyclin B1 and CDK1). (D and E) AIL inhibited the expression of STAT3 and JAK proteins. (F) Changes in JAK and STAT3 mRNA levels in the two CRC cell lines treated with AIL. Data are presented as the mean ± standard deviation, n=3. *P<0.05, **P<0.01, ***P<0.001 and ****P<0.0001, vs. control (no treatment). AIL, Ailanthone; JAK, Janus kinase; STAT3, signal transducer and activator of transcription 3.

caspase cascade pathway (15). Therefore, to further confirm this, the effects of AIL on cytochrome *c* were examined using western blot analysis. The results revealed that AIL increased the level of cytochrome *c* in the cytoplasm and decreased its expression level in the mitochondria (Fig. 4B and C). These results indicate that AIL promoted the mitochondrial-mediated apoptosis of CRC cells.

AIL induces cell cycle arrest by regulating cell cycle regulatory proteins. To investigate whether the

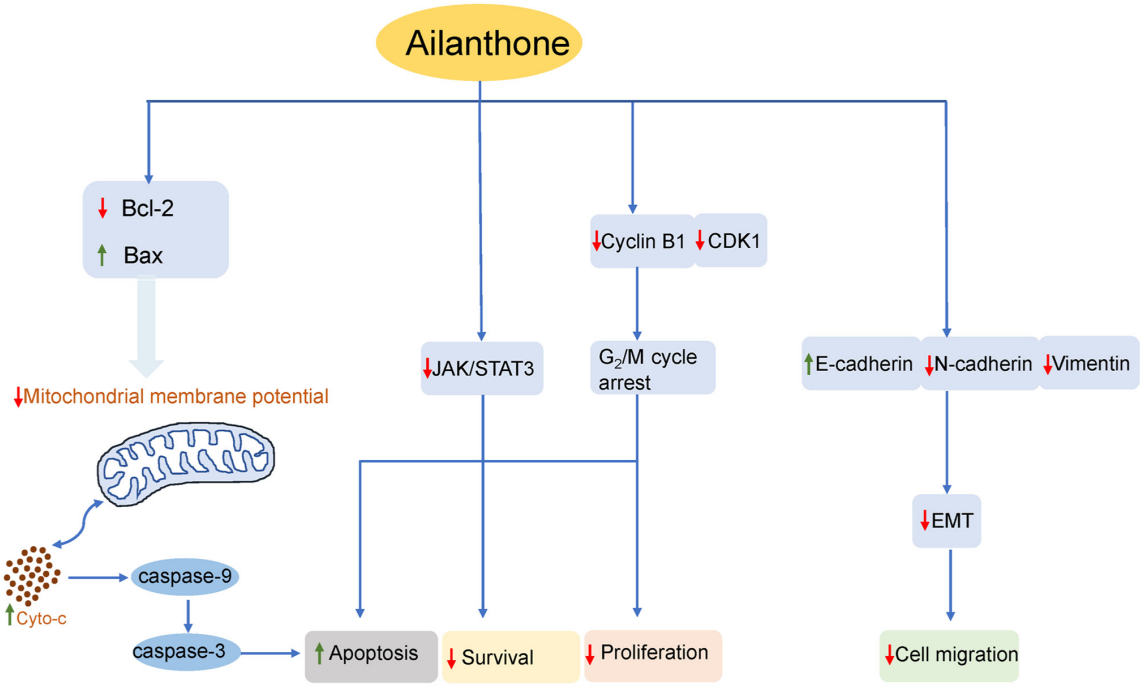

Figure 6. Mechanisms involved in the suppressive effects of Ailanthone on the activity of human colorectal cancer cells. Bcl-2, B cell lymphoma-2; Bax, Bcl-2-associated X; JAK, Janus kinase; STAT3, signal transducer and activator of transcription 3; EMT, epithelial-mesenchymal transition.

anti-proliferative effects of AIL on CRC cells were triggered by cell cycle arrest, the cell cycle phase ratio was measured using flow cytometry with DNA staining solution. As illustrated in Fig. 5A, compared with the control, AIL treatment induced the significant accumulation of cells in the G_2/M phase. The percentage of HCT116 cells in the G_2/M phase significantly increased with the increasing AIL concentration, from 16.2±0.65 to 23.43±1.22%, and that of SW620 cells increased from 3.0±0.34 to 13.41±0.92%. To investigate the molecular mechanisms through which AIL inhibited the G_2/M transition in the tumor cells, the cells were treated with AIL and the expression of proteins involved in cell cycle regulation was then analyzed. It was found that AIL treatment decreased cyclin B1 and CDK1 expression (Fig. 5B and C).

AIL inhibits JAK/STAT3 pathway activation in CRC cells. JAK/STAT3 is an important signaling pathway related to the occurrence and development of cancer. This pathway can be abnormally activated by a variety of upstream signals in cells, can regulate EMT-related genes, and is closely related to tumor proliferation, invasion, metastasis and angiogenesis (16,17). It has been confirmed that the activation of this pathway is directly related to the development of CRC (18). The present study found that AIL treatment inhibited JAK3 and STAT3 expression in the two CRC cell lines (Fig. 5D and E). Furthermore, the changes in JAK and STAT3 gene levels were detected using RT-qPCR. The results revealed that AIL inhibited the expression of the JAK and STAT3 genes in the HCT116 and SW620 cells (Fig. 5F).

Discussion

Medicinal plants have long been used in cancer treatment. Countries, such as China, Japan and Thailand have used traditional medicinal plants in the treatment of cancer for thousands of years (19). Several antitumor drugs that have been clinically used are derived from plants and have significantly prolonged the survival time of patients. For example, vincristine can be used in the treatment of leukemia (20), lymphoma (21), breast cancer (22), lung cancer (23) and pediatric solid tumors (24); paclitaxel has also been used in the treatment of ovarian, breast, lung, bladder cancer and head and neck tumors (25); docetaxel has been used in the treatment of breast (26) and lung cancer (27); in addition, irinotecan has been used in the treatment of CRC and lung cancer (28). *Ailanthus altissima* has a long history in China as a medicinal plant. AIL, one of the primary active quassinoids in *Ailanthus altissima*, has also been reported to possess certain anticancer properties in numerous *in vitro* studies (8,9,11,29,30). However, the antitumor activity of AIL against human lCRC and its mechanisms of action have not yet been elucidated. Therefore, the aim of the present study was to examine the effects of AIL on human CRC and to elucidate the underlying molecular mechanisms. To the best of our knowledge, the present study demonstrates for the first time that AIL inhibits the proliferation of CRC cells *in vitro*. The present study also revealed the molecular mechanisms through which AIL affects CRC cells and further evaluated the toxicity of AIL to normal intestinal epithelial cells (NCM460); 5-FU was used as a positive control to reflect the advantages of AIL.

The findings of the present study demonstrated that AIL suppressed the growth of HCT116 and SW620 cells in a concentration- and time-dependent manner. In addition, the inhibitory effects of AIL on the proliferation of NCM460 cells, as well as its cytotoxic effects were less prominent than those on the HCT116 and SW620, indicating that AIL exhibited a greater sensitivity to tumor cells. Moreover, when comparing

the IC50 values of AIL and 5-FU, it was found that AIL and 5-FU had a similar cytotoxicity.

The majority of the cells in the body of healthy individuals are in a quiescent phase, and cells will only re-enter the cycle when and where they are needed. The dysregulation of cell cycle progression is also considered a common characteristic of cancer, which may lead to excessive or uncontrolled cell proliferation (31). Therefore, targeting the regulatory components of the cell cycle machinery is an important strategy for the treatment of human malignancies. As previously demonstrated, AIL induced the G_0/G_1 and G_2/M phase arrest of B16 and A375 melanoma cells by downregulating cyclin E and cyclin B expression (9). In hepatocellular carcinoma, AIL has been shown to induce the G_0/G_1 phase arrest of Huh7 cells by downregulating the expression of cyclin D, cyclin E, and CDK2, CDK4 and CDK6 (13). The present study indicated that AIL induced the G_2/M cycle arrest of HCT116 and SW620 CRC cells by downregulating the levels of positive regulators of the G_2/M phase (cyclin B and CDK1), and inhibiting cell proliferation.

Apoptosis, also known as programmed cell death, is an important terminal pathway of multicellular biological cells. In the majority of eukaryotic cells, there are two major apoptotic pathways: The death receptor pathway and the mitochondrial pathway. The process is highly regulated, which can eliminate damaged cells (such as DNA-damaged cells) and senescent cells in an orderly and effective manner to maintain the stability of the internal environment (32). The evasion of cell death is one of the important characteristics of the malignant transformation of normal cells to tumor cells (33). It has been found that a variety of novel drugs, such as Bcl-2 inhibitors (ABT-263, ABT-737, GX15-070 and fenretinide) (34), caspase activators (35), caspase inducers (apoptin) (36), etc. can induce tumor cell apoptosis. In the present study, it was found that AIL induced cell apoptosis through the mitochondrial pathway. The Bcl-2 protein family is considered to be a switch that controls the mitochondrial apoptotic pathway by affecting the permeability of the mitochondrial membrane (37). To further investigate the underlying molecular mechanisms of AIL-induced apoptosis, the protein expression levels of Bcl-2, Bax were detected in CRC cells treated with AIL. The results of western blot analysis revealed that AIL increased the Bax and decreased Bcl-2 expression, which altered the permeability of the mitochondrial membrane, resulting in an increase in the amount of cytochrome *c* in the cytosol, finally inducing caspase-3 and -9 activation, as well as apoptosis.

STAT family members are usually divided into two subgroups. The first group is involved in T-cell development and IFN-γ signal transduction and mainly includes STAT2, STAT4 and STAT6. The second group is related to embryogenesis, breast development and tumor occurrence, and mainly includes STAT1, STAT3 and STAT5 (38). Among them, STAT3 is considered to be highly related to tumor development. It can regulate cell proliferation-related genes (c-Myc and cyclin D1), anti-apoptotic genes (Mcl1, Bcl-xL, Bcl-2 and survivin), and angiogenesis-related genes (BFGF, HIF-1α, VEGF and HGF) and metastasis and EMT process-related genes [Snail, Slug, Twist1, Vimentin, matrix metalloproteinase (MMP)2, MMP9 and HMGB1] (16,39). The STAT3 pathway is closely related to the occurrence and development of CRC, and the activation of this pathway can affect the progression of CRC via several mechanisms (40,41). The activation of STAT3 signaling can drive Th17 cells in CRC to secrete cytokines (IL-17A, IL-17F, IL-21 and IL-22) to promote tumor angiogenesis and tumorigenesis (42). c-Myc is an important transcription factor that can affect a variety of cell biological functions, such as proliferation, differentiation, growth and apoptosis. The high expression of c-Myc is common in CRC, which is often associated with a poor prognosis (43). The continuous activation of STAT3 activates c-Myc to promote tumor progression. Furthermore, the STAT3 signaling pathway can upregulate the expression of the positive cell cycle regulatory protein, cyclin D1 (44). STAT3 can induce the expression of the anti-apoptotic proteins, Bcl-2, Mcl-1, survivin and Bcl-xL, to inhibit apoptosis and promote proliferation (45,46). The activation of the STAT3 signaling pathway can also induce the expression of MMPs and EMT regulatory factors (Snail and Twist1), and can downregulate E-cadherin and upregulate vimentin expression, thereby enhancing the invasiveness and metastatic ability of CRC (47,48). Therefore, targeting the STAT3 signaling pathway may be a feasible and effective treatment strategy. A number of clinical studies using STAT3 pathway-targeting drugs have been performed, such as IL-6 inhibitors (siltuximab) (49), JAK inhibitors (ruxolitinib and itacitinib) (50,51) and STAT3 inhibitors (OPB-31121, GRIM19, AZD9150 and TTI-101) (52-55). In addition, certain naturally derived compounds (piperine, matrine, luteolin, curcumin, etc.) have been confirmed to target the STAT3 signaling pathway and to exert anticancer effects (56-59). In the present study, it was found that AIL significantly inhibited the expression of JAK and STAT3 proteins in HCT116 and SW620CRC cells. Furthermore, specific primers for JAK and STAT3 were designed. In addition, the changes in the mRNA levels of JAK and STAT3 were examined following treatment with AIL using RT-qPCR, and found that AIL inhibited the expression of the two genes. It was thus demonstrated that AIL inhibited the activation of the JAK/STAT3 signaling pathway in the HCT116 and SW620 CRC cell lines. In addition, compared with the control group, the mRNA levels of JAK1 and STAT3 were significantly decreased. All these results indicate that AIL inhibits the activation of the JAK/STAT3 signaling pathway in the HCT116 and SW620 CRC cell lines.

In conclusion, the findings of the present study indicated that AIL inhibited the proliferation and migration of HCT116 and SW620 CRC cells *in vitro*, promoted apoptosis and exerted inhibitory effects on tumor-related signaling pathways (Fig. 6). These results indicate that AIL may have potential for use in the treatment of CRC; thus, it may be worthy of further investigation.

Acknowledgements

Not applicable.

Funding

The present study was funded by the Traditional Chinese Medicine Science and Technology Project of Zhejiang Province (grant no. 2018ZA109), the Medical and Health Science and Technology Project of Zhejiang Province

(grant no. 2018ZH026), the Natural Science Foundation of Ningbo (grant nos. 2016A610157 and 2018A610371) and the Science and Technology Projects of Zhejiang Province (grant no. LGF19H030007).

Availability of data and materials

The datasets used and/or analyzed during the current study are available from the corresponding author on reasonable request.

Authors' contributions

XY and ZY conceived and supervised the whole study. HD and XY performed the experiments and the data analysis. HD drafted the manuscript. XY and ZY revised the manuscript. HD and XY confirm the authenticity of all the raw data. All authors agree to be accountable for all aspects of the work ensuring integrity and accuracy, and all authors have read and approved the final manuscript.

Ethics approval and consent to participate

Not applicable.

Patient consent for publication

Not applicable.

Competing interests

The authors declare that they have no competing interests.

References

1. Bray F, Ferlay J, Soerjomataram I, Siegel RL, Torre LA and Jemal A: Global cancer statistics 2018: GLOBOCAN estimates of incidence and mortality worldwide for 36 cancers in 185 countries. CA Cancer J Clin 68: 394-424, 2018.
2. Nikolaou M, Pavlopoulou A, Georgakilas AG and Kyrodimos E: The challenge of drug resistance in cancer treatment: a current overview. Clin Exp Metastasis 35: 309-318, 2018.
3. Wang P, Yang HL, Yang YJ, Wang L and Lee SC: Overcome cancer cell drug resistance using natural products. Evid Based Complement Alternat Med 2015: 767136, 2015.
4. Alves IA, Miranda HM, Soares LA and Randau KP: Simaroubaceae family: Botany, chemical composition and biological activities. Rev Bras Farmacogn 24: 481-501, 2014.
5. Ding H, Yu X, Hang C, Gao K, Lao X, Jia Y and Yan Z: Ailanthone: A novel potential drug for treating human cancer. Oncol Lett 20: 1489-1503, 2020.
6. Casinovi CG, Ceccherelli P, Grandolini G and Bellavita V: On the structure of Ailanthone. Tetrahedron Lett 5: 3991-3997, 1964.
7. Ishibashi M, Tsuyuki T, Murae T, Hirota H, Takahashi T, Itai A and Iitaka Y: Constituents of the root bark of *Ailanthus altissima* swingle. Isolation and X-ray crystal structures of shinjudilactone and shinjulactone C and conversion of ailanthone into shinjudilactone. Bull Chem Sok Jpn 56: 3683-3693, 1983.
8. Hou S, Cheng Z, Wang W, Wang X and Wu Y: Ailanthone exerts an antitumor function on the development of human lung cancer by upregulating microRNA-195. J Cell Biochem 120: 10444-10451, 2019.
9. Liu W, Liu X, Pan Z, Wang D, Li M, Chen X, Zhou L, Xu M, Li D and Zheng Q: Ailanthone induces cell cycle arrest and apoptosis in melanoma B16 and A375 cells. Biomolecules 9: 275, 2019.
10. Daga M, Pizzimenti S, Dianzani C, Cucci MA, Cavalli R, Grattarola M, Ferrara B, Scariot V, Trotta F and Barrera G: Ailanthone inhibits cell growth and migration of cisplatin resistant bladder cancer cells through down-regulation of Nrf2, YAP, and c-Myc expression. Phytomedicine 56: 156-164, 2019.
11. Chen Y, Zhu L, Yang X, Wei C, Chen C, He Y and Ji Z: Ailanthone induces G2/M cell cycle arrest and apoptosis of SGC-7901 human gastric cancer cells. Mol Med Rep 16: 6821-6827, 2017.
12. He Y, Peng S, Wang J, Chen H, Cong X, Chen A, Hu M, Qin M, Wu H, Gao S, *et al*: Ailanthone targets p23 to overcome MDV3100 resistance in castration-resistant prostate cancer. Nat Commun 7: 13122, 2016.
13. Zhuo Z, Hu J, Yang X, Chen M, Lei X, Deng L, Yao N, Peng Q, Chen Z, Ye W and Zhang D: Ailanthone inhibits Huh7 cancer cell growth via cell cycle arrest and apoptosis in vitro and in vivo. Sci Rep 5: 16185, 2015.
14. Livak KJ and Schmittgen TD: Analysis of relative gene expression data using real-time quantitative PCR and the 2(-Delta Delta C(T)) method. Methods 25: 402-408, 2001.
15. Danial NN and Korsmeyer SJ: Cell death: Critical control points. Cell 116: 205-219, 2004.
16. Liu RY, Zeng Y, Lei Z, Wang L, Yang H, Liu Z, Zhao J and Zhang HT: JAK/STAT3 signaling is required for TGF-β-induced epithelial-mesenchymal transition in lung cancer cells. Int J Oncol 44: 1643-1651, 2014.
17. Huang W, Yu LF, Zhong J, Wu W, Zhu JY, Jiang FX and Wu YL: Stat3 is involved in angiotensin II-induced expression of MMP2 in gastric cancer cells. Dig Dis Sci 54: 2056-2062, 2009.
18. Xiong H, Zhang ZG, Tian XQ, Sun DF, Liang QC, Zhang YJ, Lu R, Chen YX and Fang JY: Inhibition of JAK1, 2/STAT3 signaling induces apoptosis, cell cycle arrest, and reduces tumor cell invasion in colorectal cancer cells. Neoplasia 10: 287-297, 2008.
19. Qi F, Zhao L, Zhou A, Zhang B, Li A, Wang Z and Han J: The advantages of using traditional Chinese medicine as an adjunctive therapy in the whole course of cancer treatment instead of only terminal stage of cancer. Biosci Trends 9: 16-34, 2015.
20. Bezwoda WR, MacDonald DF, Gear JS, Derman DP, Bothwell TH, Sqi S, Hurwitz S and Lewis D: Combination chemotherapy including bleomycin in the treatment of advanced Hodgkin's disease. S Afr Med J 53: 369-373, 1978.
21. Durant JR, Gams RA, Bartolucci AA and Dorfman RF: BCNU with and without cyclophosphamide, vincristine, and prednisone (COP) and cycle-active therapy in non-Hodgkin's lymphoma. Cancer Treat Rep 61: 1085-1096, 1977.
22. Wong MY and Chiu GN: Liposome formulation of co-encapsulated vincristine and quercetin enhanced antitumor activity in a trastuzumab-insensitive breast tumor xenograft model. Nanomedicine 7: 834-840, 2011.
23. Munker S, Vogelhuber M, Bornschein J, Stroszczynski C, Evert M, Schlitt H, Herr W and Teufel A: EpiCO (epirubicin, cyclophosphamide and vincristine) as treatment for extrapulmonary high-grade neuroendocrine neoplasms. Z Gastroenterol 58: 133-136, 2020.
24. Büyükkapu Bay S, Kebudi R, Görgün O, Zülfikar B, Darendeliler E and Çakır FB: Vincristine, irinotecan, and temozolomide treatment for refractory/relapsed pediatric solid tumors: A single center experience. J Oncol Pharm Pract 25: 1343-1348, 2019.
25. Weaver BA: How Taxol/paclitaxel kills cancer cells. Mol Biol Cell 25: 2677-2681, 2014.
26. Caparica R, Bruzzone M, Poggio F, Ceppi M, de Azambuja E and Lambertini M: Anthracycline and taxane-based chemotherapy versus docetaxel and cyclophosphamide in the adjuvant treatment of HER2-negative breast cancer patients: A systematic review and meta-analysis of randomized controlled trials. Breast Cancer Res Treat 174: 27-37, 2019.
27. Reck M, Brahmer J, Bennett B, Taylor F, Penrod JR, DeRosa M, Dastani H, Spigel DR and Gralla RJ: Evaluation of health-related quality of life and symptoms in patients with advanced non-squamous non-small cell lung cancer treated with nivolumab or docetaxel in CheckMate 057. Eur J Cancer 102: 23-30, 2018.
28. da Rocha AB, Lopes RM and Schwartsmann G: Natural products in anticancer therapy. Curr Opin Pharmacol 1: 364-369, 2001.
29. Zhang Y, Zhang C and Min D: Ailanthone up-regulates miR-449a to restrain acute myeloid leukemia cells growth, migration and invasion. Exp Mol Pathol 108: 114-120, 2019.
30. Ni Z, Yao C, Zhu X, Gong C, Xu Z, Wang L, Li S, Zou C and Zhu S: Ailanthone inhibits non-small cell lung cancer cell growth through repressing DNA replication via downregulating RPA1. Br J Cancer 117: 1621-1630, 2017.
31. Hanahan D and Weinberg RA: Hallmarks of cancer: The next generation. Cell 144: 646-674, 2011.
32. Fuchs Y and Steller H: Programmed cell death in animal development and disease. Cell 147: 742-758, 2011.

33. Hanahan D and Weinberg RA: The hallmarks of cancer. Cell 100: 57-70, 2000.
34. Kang MH and Reynolds CP: Bcl-2 inhibitors: Targeting mitochondrial apoptotic pathways in cancer therapy. Clin Cancer Res 15: 1126-1132, 2009.
35. Philchenkov A, Zavelevich M, Kroczak TJ and Los M: Caspases and cancer: Mechanisms of inactivation and new treatment modalities. Exp Oncol 26: 82-97, 2004.
36. Rohn JL and Noteborn MH: The viral death effector apoptin reveals tumor-specific processes. Apoptosis 9: 315-322, 2004.
37. Terrano DT, Upreti M and Chambers TC: Cyclin-dependent kinase 1-mediated Bcl-xL/Bcl-2 phosphorylation acts as a functional link coupling mitotic arrest and apoptosis. Mol Cell Biol 30: 640-656, 2010.
38. Siveen KS, Sikka S, Surana R, Dai X, Zhang J, Kumar AP, Tan BK, Sethi G and Bishayee A: Targeting the STAT3 signaling pathway in cancer: Role of synthetic and natural inhibitors. Biochim Biophys Acta 1845: 136-154, 2014.
39. Lee H, Jeong AJ and Ye SK: Highlighted STAT3 as a potential drug target for cancer therapy. BMB Rep 52: 415-423, 2019.
40. Zeng J, Tang ZH, Liu S and Guo SS: Clinicopathological significance of overexpression of interleukin-6 in colorectal cancer. World J Gastroenterol 23: 1780-1786, 2017.
41. Waldner MJ and Neurath MF: Master regulator of intestinal disease: IL-6 in chronic inflammation and cancer development. Semin Immunol 26: 75-79, 2014.
42. Velikova TV, Miteva L, Stanilov N, Spassova Z and Stanilova SA: Interleukin-6 compared to the other Th17/Treg related cytokines in inflammatory bowel disease and colorectal cancer. World J Gastroenterol 26: 1912-1925, 2020.
43. Lee KS, Kwak Y, Nam KH, Kim DW, Kang SB, Choe G, Kim WH and Lee HS: c-MYC copy-number gain is an independent prognostic factor in patients with colorectal cancer. PLoS One 10: e0139727, 2015.
44. Leslie K, Lang C, Devgan G, Azare J, Berishaj M, Gerald W, Kim YB, Paz K, Darnell JE, Albanese C, *et al*: Cyclin D1 is transcriptionally regulated by and required for transformation by activated signal transducer and activator of transcription 3. Cancer Res 66: 2544-2552, 2006.
45. Lee DH, Sung KS, Bartlett DL, Kwon YT and Lee YJ: HSP90 inhibitor NVP-AUY922 enhances TRAIL-induced apoptosis by suppressing the JAK2-STAT3-Mcl-1 signal transduction pathway in colorectal cancer cells. Cell Signal 27: 293-305, 2015.
46. Tian Y, Ye Y, Gao W, Chen H, Song T, Wang D, Mao X and Ren C: Aspirin promotes apoptosis in a murine model of colorectal cancer by mechanisms involving downregulation of IL-6-STAT3 signaling pathway. Int J Colorectal Dis 26: 13-22, 2011.
47. Liu H, Ren G, Wang T, Chen Y, Gong C, Bai Y, Wang B, Qi H, Shen J, Zhu L, *et al*: Aberrantly expressed Fra-1 by IL-6/STAT3 transactivation promotes colorectal cancer aggressiveness through epithelial-mesenchymal transition. Carcinogenesis 36: 459-468, 2015.
48. Han C, Sun B, Zhao X, Zhang Y, Gu Q, Liu F, Zhao N and Wu L: Phosphorylation of STAT3 promotes vasculogenic mimicry by inducing epithelial-to-mesenchymal transition in colorectal cancer. Technol Cancer Res Treat 16: 1209-1219, 2017.
49. Angevin E, Tabernero J, Elez E, Cohen SJ, Bahleda R, van Laethem JL, Ottensmeier C, Lopez-Martin JA, Clive S, Joly F, *et al*: A phase I/II, multiple-dose, dose-escalation study of siltuximab, an anti-interleukin-6 monoclonal antibody, in patients with advanced solid tumors. Clin Cancer Res 20: 2192-2204, 2014.
50. Fogelman D, Cubillo A, García-Alfonso P, Mirón MLL, Nemunaitis J, Flora D, Borg C, Mineur L, Vieitez JM, Cohn A, *et al*: Randomized, double-blind, phase two study of ruxolitinib plus regorafenib in patients with relapsed/refractory metastatic colorectal cancer. Cancer Med 7: 5382-5393, 2018.
51. Beatty GL, Shahda S, Beck T, Uppal N, Cohen SJ, Donehower R, Gabayan AE, Assad A, Switzky J, Zhen H and Von Hoff DD: A phase Ib/II study of the JAK1 inhibitor, itacitinib, plus nab-paclitaxel and gemcitabine in advanced solid tumors. Oncologist 24: 14-e10, 2019.
52. Oh DY, Lee SH, Han SW, Kim MJ, Kim TM, Kim TY, Heo DS, Yuasa M, Yanagihara Y and Bang YJ: Phase I study of OPB-31121, an oral STAT3 inhibitor, in patients with advanced solid tumors. Cancer Res Treat 47: 607-615, 2015.
53. Okamoto T, Inozume T, Mitsui H, Kanzaki M, Harada K, Shibagaki N and Shimada S: Overexpression of GRIM-19 in cancer cells suppresses STAT3-mediated signal transduction and cancer growth. Mol Cancer Ther 9: 2333-2343, 2010.
54. Hong D, Kurzrock R, Kim Y, Woessner R, Younes A, Nemunaitis J, Fowler N, Zhou T, Schmidt J, Jo M, *et al*: AZD9150, a next-generation antisense oligonucleotide inhibitor of STAT3 with early evidence of clinical activity in lymphoma and lung cancer. Sci Transl Med 7: 314ra185, 2015.
55. Bharadwaj U, Kasembeli MM, Robinson P and Tweardy DJ: Targeting janus kinases and signal transducer and activator of transcription 3 to treat inflammation, fibrosis, and cancer: Rationale, progress, and caution. Pharmacol Rev 72: 486-526, 2020.
56. Song L, Wang Y, Zhen Y, Li D, He X, Yang H, Zhang H and Liu Q: Piperine inhibits colorectal cancer migration and invasion by regulating STAT3/Snail-mediated epithelial-mesenchymal transition. Biotechnol Lett 42: 2049-2058, 2020.
57. Zhou H, Chen S, Yang Y, Yang C, Chen D, Yao Z and Sun B: Matrine enhances the efficacy of adriamycin chemotherapy in osteosarcoma cells by the STAT3 pathway. Anticancer Drugs 30: 1006-1012, 2019.
58. Cummins CB, Wang X, Nunez Lopez O, Graham G, Tie HY, Zhou J and Radhakrishnan RS: Luteolin-mediated inhibition of hepatic stellate cell activation via suppression of the STAT3 pathway. Int J Mol Sci 19: 1567, 2018.
59. Hayakawa T, Yaguchi T and Kawakami Y: Enhanced anti-tumor effects of the PD-1 blockade combined with a highly absorptive form of curcumin targeting STAT3. Cancer Sci 111: 4326-4335, 2020.